

1 An early warning sign: trophic structure changes in the oceanic Gulf of Mexico from 2011-2018
2

3 Matthew S. Woodstock^{a*}, Tracey T. Sutton^b, Tamara Frank^b, Yuying Zhang^a

4 Affiliations:

5 ^aDepartment of Biological Sciences, Oceans and Coastal Division, Institute of Environment,
6 Florida International University 3000 NE 151st St. North Miami, FL

7 ^bDepartment of Marine and Environmental Sciences, Nova Southeastern University 8000 N.
8 Ocean Dr., Dania Beach, FL.

9 Corresponding Author*: Matthew S. Woodstock; mwood078@fiu.edu

10 Co-Author Emails: Tracey T. Sutton: tsutton1@nova.edu; Tamara Frank: tfrank1@nova.edu;

11 Yuying Zhang: yzhang13@fiu.edu

12 Running Head: Gulf of Mexico trophic structure

13 Abstract

14 Ecosystem-based modeling is rapidly becoming an established technique to investigate the
15 health and stability of ecosystems. In the Gulf of Mexico, ecosystem models are applied to
16 neritic systems, but less focus has been placed on the oceanic domain. Since 2011, severe
17 declines have been observed in many micronekton groups that occupy the mesopelagic zone
18 (200 – 1000 m depth). Here we present an ecosystem model for the oceanic northern Gulf of
19 Mexico for the year 2011, simulate that model according to micronekton trends through 2018,
20 and quantify the top-down and bottom-up impacts that each functional group has on one another.
21 These trends were examined to determine whether interactions between the two groups have
22 changed directionally over time. In 2011, zooplankton (trophic level =2) occupied greater than

23 one-third of the total metazoan biomass, and also 40% of the total energy throughput ascended to
24 higher trophic levels in the system. Of the 1849 possible functional group interactions (most of
25 which are indirect), approximately 27% showed significant changes between 2011 and 2018,
26 which were related to shifts in biomass and diet throughout the simulation. Direct top-down
27 interactions changed more frequently than other types of trophic relationships. The frequency of
28 direct changes that occurred in the simulation was not observed evenly among all functional
29 groups, as opposed to indirect interactions. These changes between functional group interactions
30 can be used to further examine potential shifts in the trophic structure of marine ecosystems
31 under various forcing scenarios.

32

33 Keywords: Gulf of Mexico; Food Web; Ecosystem Modeling; Mesopelagic; Network Analysis;
34 Trophic Structure

35

36

37 1. Introduction

38 The open ocean is Earth's largest biome. This complex and dynamic consortium of
39 ecosystems is subject to continual anthropogenic inputs and disturbances. Globally,
40 anthropogenic stressors have influenced commercial fisheries stocks (Hilborn, 2011), non-
41 commercial species' populations (Guinotte and Fabry, 2008), and abiotic drivers (Hoegh-
42 Goldberg and Bruno, 2010) in marine systems. Increased stress exerted on an ecosystem reduces
43 the system's stability and resiliency towards future disturbances (Costanza and Magaeu, 1999).
44 In order to examine the health and stability of an ecosystem, a multi-species modeling approach
45 is useful to track the interactions of many species within the same model. Ecosystem modeling is
46 a tool that combines information regarding all known biotic and abiotic components of an
47 ecosystem with the goal of quantifying ecosystem services and food-web topology (Levin et al.,
48 2008). In ecosystem models, both direct (trophic connection exists) and indirect interactions (no
49 trophic interaction between species) can be investigated (Monaco and Ulanowicz, 1997).
50 However, ecosystem models require many input values, and simulations involve the changing of
51 many parameters. This increases the uncertainty of an ecosystem model when compared to a
52 single-species model. Due to a lack of sufficient data, there are few ecosystem models for the
53 oceanic realm (seaward of the 200-m isobath) when compared to neritic zones (Webb et al.,
54 2010). A lack of ecosystem models hinders our ability to predict shifts in the trophic structure of
55 oceanic ecosystems over time.

56 The trophic structure of an ecosystem is often classified as a series of "top-down" and
57 "bottom-up" interactions among species and is associated with predator and prey abundances
58 within the system (Verity and Smetacek, 1996). Fluctuations in the population size of a predator
59 species may have an impact on the population size of a prey species, but this effect is not equal

60 across all prey of a single predator species (Worm and Myers, 2003). Ulanowicz and Puccia
61 (1990) developed the mixed trophic impact measurement (MTI): a metric to determine the effect
62 an infinitesimal increase in the population size of one functional group would have on each other
63 functional group within an ecosystem. This index ranges from -1 to 1, where large negative
64 values indicate top-down feedback and large positive values indicate bottom-up feedback. MTI
65 has been used extensively in ecosystem models to recognize keystone species (Libralato et al.,
66 2006), important trophic connections (Sagarese et al., 2017), and the importance of fishing
67 pressure towards the future status of a fishery (Walters et al., 1997). Given that the MTI is a
68 measure of the relative effect of one functional group on another within the ecosystem, changes
69 in MTIs among multiple pairs of functional groups over time indicate changes to the system's
70 trophic structure. When simulating an ecosystem across time, it may be valuable to model a
71 series of individual time steps as static ecosystems and analyze this positioning as a time series.
72 This method is usually developed for ecosystem-level indicators, such as biomass (Coll and
73 Steenbeek, 2017), yield (Coll et al., 2008), and trophic level (Shannon et al., 2014). Calculating
74 MTI at each time step in the simulation may reveal potential trends in the top-down/bottom-up
75 impacts one species exerts on another (relative to other species within the model).

76 Akin to other low-latitude systems, large finfishes (e.g., tunas, billfishes, and sharks) are the
77 predominant apex predators in the epipelagic (0 – 200 m depth) Gulf of Mexico (GoM,
78 hereafter), while marine mammals exist in lower abundances. Many of these upper trophic level
79 predators make routine dives into mesopelagic depths to prey upon micronekton assemblages
80 (Watwood et al., 2006; Wilson and Block, 2009). Many mesopelagic organisms (particularly
81 those in the deep-scattering layer) ascend into the epipelagic zone during nighttime to prey upon
82 zooplankton or other mesopelagic migrators and descend back into mesopelagic depths during

83 the daytime to avoid predators (Frost and McCrone, 1978). Deeper-dwelling pelagic predators
84 (e.g., swordfishes) make a diel vertical migration into the epipelagic zone during the night as
85 well, presumably following micronekton prey (Lerner et al., 2013). However, the micronekton
86 assemblage is diverse, and predators are likely not confined to a single prey source. Instead,
87 upper trophic level predators in the upper ocean are likely opportunistically feeding on the entire
88 assemblage, suggesting the ecosystem may be resilient to severe declines in a singular functional
89 group (Ménard et al., 2006). Micronekton feed on diverse zooplankton and micronekton
90 assemblages in a manner that may be taxon- or size-class-specific to partition resources among
91 species (Hopkins and Sutton, 1998). Overall, the food web of the oceanic GoM is complex, with
92 depth layers connected by vertical migrations. Changes in the population size of functional
93 groups within the ecosystem may alter the trophic structure of the system.

94 Recently, a large emphasis has been placed on ecosystem-based management in the northern
95 GoM (Grüss et al., 2016). This emphasis can be attributed to the large amounts of data collected
96 since the 2010 *Deepwater Horizon* oil spill and an increase in data sharing capabilities through
97 online data repositories, such as GRIIDC (www.data.gulfresearchinitiative.org). These models
98 have focal points that address ecosystem restoration (de Mutsert et al., 2012), harmful algal
99 blooms (Perryman et al., 2020), hypoxia (de Mutsert et al., 2016), fishery policy decisions
100 (Chagaris et al., 2015), and trophic interactions (Geers et al., 2016). Ecosystem models
101 constructed in the GoM have primarily focused on the coastal realm, with just a few exceptions
102 expanding into the open ocean (Vidal and Pauly, 2004; Ainsworth et al., 2015). Rigorous data
103 collection of non-commercial species in the open ocean since 2011 has filled data gaps,
104 providing data necessary to develop an ecosystem model for this domain (Sutton et al., 2020). A
105 model devoted to the offshore GoM would highlight the importance of micronekton as prey

106 resources and predators of other organisms in the ecosystem, as is apparent in other oceanic
107 systems (Griffiths et al., 2013; Choy et al., 2016).

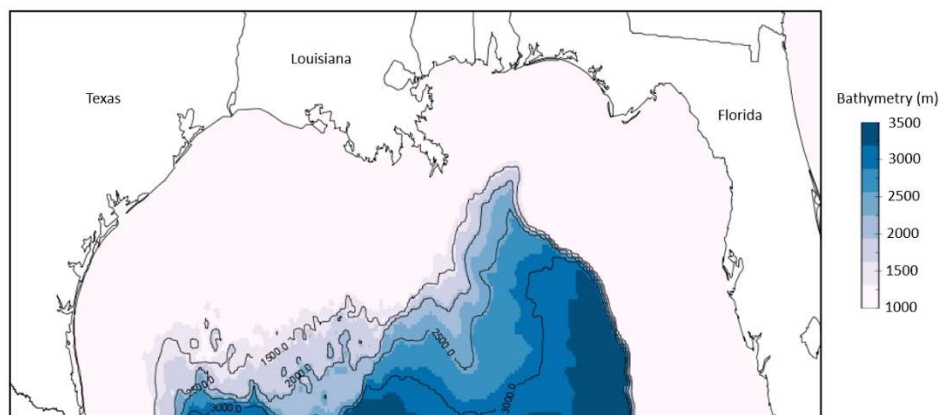
108 In this study, we present the first ecosystem model in the northern GoM devoted to the
109 offshore waters seaward of the 1000-m isobath. The model is simulated from 2011 to 2018,
110 using observed trends in mesopelagic micronekton as the driver of the simulation. We explore
111 the uncertainty in input parameters and use this potential error to provide confidence intervals
112 towards model output results. The trophic structure of the ecosystem is characterized in the
113 context of relative top-down and bottom-up relationships among species. We estimate how these
114 trophic interactions have changed from 2011 to 2018. Finally, we discuss these changes in the
115 context of ecosystem health and stability.

116 2. Methods

117 2.1. Model structure

118 The modeled area encompasses the GoM portion of the U.S. Exclusive Economic Zone,
119 seaward of the 1000-m isobath, approximately 350,000 km² (Zeller and Pauly, 2015; Figure 1).
120 The vertical domain of the model region is from the surface to 1000-m depth. The functional
121 groups in the ecosystem model included all species that occupy the ecosystem at any time
122 throughout the year. Nine species: yellowfin tuna (*Thunnus albacares*), blue marlin (*Makaira*
123 *nigricans*), bigeye tuna (*Thunnus obesus*), white marlin (*Kajikia albidus*), swordfish (*Xiphias*
124 *gladius*), sailfish (*Istiophorus albicans*), bluefin tuna (*Thunnus thynnus*), albacore tuna (*Thunnus*
125 *alalunga*), and skipjack tuna (*Katsuwonus pelamis*) were each divided into two-stage multi-
126 stanza groups (juvenile and adult) to account for ontogenetic changes in diet and fishing
127 selectivity. Larval conspecifics were included in the juvenile life stage, as tuna and billfish larval
128 stages are much shorter than one year and growth rates are rapid (Fromentin and Powers, 2005;

129 Sponaugle et al., 2010). The age of each multi-stanza division was determined by the age at
130 maturity referenced in stock assessments. Roundscale spearfish (*Tetrapturus georgii*) is included
131 with white marlin because of difficulties in distinguishing between the two species by fishers
132 (Shivji et al., 2006). Mesopelagic fishes included the four biomass-dominant fish families in the
133 GoM (Myctophidae, Sternoptychidae, Gonostomatidae, and Stomiidae). Mesopelagic fishes from
134 other families were aggregated based on the known (Hopkins et al., 1996) or assumed trophic
135 positions. Juvenile neritic fishes that either migrate or are advected offshore by currents were
136 included in the epipelagic forage feeder group, as this would be their ecological role. Aggregate
137 groups of invertebrates and primary producers were necessary to complete the food web. The
138 resulting model consists of 42 functional groups, including three marine mammal groups, sea
139 turtles, seabirds, 29 fish groups (10 of which are larval or juvenile), six invertebrate groups, one
140 primary producer, and one detritus group. Additionally, one fishery is included in the model.



141
142 **Figure 1.** Map of the model domain. This model includes the area of the U.S. Exclusive
143 Economic Zone of the northern Gulf of Mexico, seaward of the 1000-m isobath. Color shading is
144 included to show bathymetry. The average depth of the model domain is 2,297 m.

145

146 2.2 Ecopath with Ecosim

147 Ecopath with Ecosim (EwE) is a mass-balanced ecosystem software that assumes the
148 ecosystem is in equilibrium. EwE was initially developed as a method to provide information
149 about the standing stock of functional groups and the flow of energy throughout an ecosystem
150 (Polovina, 1984). Since its initial release, EwE has undergone extensive development with the
151 inclusion of additional plug-in procedures (Steenbeek et al., 2016), but the original framework
152 still exists in the current software. Two master equations control the mass-balance assumption
153 within Ecopath: One describes production, and the second describes energy balance (*sensu*
154 Christensen et al., 2008). Four Ecopath parameters are necessary for each group: Biomass (B),
155 Production/Biomass (P/B), Consumption/Biomass (Q/B), and Ecotrophic Efficiency (EE; Table
156 1). Ecotrophic efficiency is defined as the proportion of production that is used within the system
157 and is best calculated as an estimated parameter when all other information is known. A Biomass
158 Accumulation (BA) parameter can be included to reflect population trends leading into the initial
159 model year and can increase the reliability of model results in data-limited ecosystems
160 (Natugonza et al., 2020). Ecopath once required the assumption of a steady state (Polovina,
161 1984), but advancements have reduced this assumption so that each functional group must
162 achieve mass balance throughout each time step in the model and can otherwise be dynamic. An
163 additional input parameter is the diet composition (i.e., the proportion of annual diet by biomass)
164 of each predator group on each prey group in the model. The diet of each functional group must
165 be entered and cannot be estimated (including cohorts of multi-stanza groups). In this model, diet
166 information is provided from bibliographic sources (Supplementary Material A).

167

168 **Table 1.** Input values of the original Ecopath model. Values estimated by the software are in bold. Trophic level is derived as a
 169 fractionated value from the diet matrix.

Group No.	Group name	Trophic level	Biomass (t/km ²)	P/B (/year)	Q/B (/year)	EE	P/Q (/year)	BA rate (/year)
1	Toothed Whales	4.50	1.10E-03	0.020	4.113	0.021	0.005	-
2	Baleen Whales	4.15	2.21E-04	0.020	4.684	0.000	0.004	-
3	Dolphins	4.22	1.39E-02	0.020	14.119	0.357	0.001	-
4	Seabirds	3.76	1.66E-03	0.300	1.000	0.100	0.300	-
5	Sea Turtles	3.43	1.21E-02	0.190	0.950	0.100	0.200	-
6	Oceanic Sharks	4.63	3.11E-03	0.454	3.165	0.100	0.144	-
7	Adult Albacore	4.46	4.87E-04	0.550	11.024	0.345	0.050	2.30E-06
8	Juvenile Albacore	4.03	9.23E-04	0.750	20.819	0.361	0.036	2.30E-06
9	Adult Bigeye	4.25	2.81E-05	0.700	6.915	0.259	0.101	-9.00E-07
10	Juvenile Bigeye	3.80	1.85E-05	0.800	12.889	0.051	0.062	-9.00E-07
11	Adult Bluefin	4.07	7.07E-04	0.500	4.815	0.168	0.104	4.10E-06
12	Juvenile Bluefin	3.62	3.04E-02	0.700	9.243	0.038	0.076	4.10E-06
13	Adult Sailfish	4.05	2.99E-03	0.407	7.216	0.245	0.056	3.50E-04
14	Juvenile Sailfish	3.73	7.92E-04	0.356	12.350	0.317	0.029	3.50E-04
15	Adult Yellowfin	3.93	1.09E-01	0.477	10.820	0.058	0.044	-5.50E-03
16	Juvenile Yellowfin	3.82	1.02E-01	1.179	20.106	0.125	0.059	-5.50E-03
17	Adult Swordfish	4.15	2.46E-02	0.679	8.339	0.106	0.081	-2.40E-03
18	Juvenile Swordfish	3.56	2.50E-02	0.448	15.087	0.054	0.030	-2.40E-03
19	Adult White Marlin	4.24	5.71E-03	0.350	8.132	0.256	0.043	4.50E-05
20	Juvenile White Marlin	3.81	1.99E-04	0.550	18.358	0.093	0.030	4.50E-05
21	Adult Skipjack	3.75	3.69E-05	1.441	14.564	0.039	0.099	-8.10E-06
22	Juvenile Skipjack	3.49	5.37E-06	0.864	30.778	0.010	0.028	-8.10E-06
23	Adult Blue Marlin	4.19	1.26E-03	0.500	5.580	0.349	0.090	3.90E-05
24	Juvenile Blue Marlin	3.81	4.92E-04	0.600	10.066	0.123	0.060	3.90E-05
25	Small Tunas and Other Large Predators	4.05	6.36E-03	1.069	8.342	0.400	0.128	-
26	Dragonfishes	3.95	2.70E-03	1.119	5.595	0.800	0.200	-
27	Other Mesopelagic Zooplanktivores	3.30	2.43E-02	1.138	3.498	0.950	0.325	-

28	Epipelagic Forage Feeders	3.15	3.30E+00	1.017	22.122	0.600	0.046	-
29	Other Mesopelagic Micronektonivores	3.91	5.13E-02	0.875	2.915	0.950	0.300	-
30	Hatchetfishes	3.33	1.10E-02	4.588	15.293	0.403	0.300	-
31	Bristlemouths	3.27	7.92E-02	3.386	11.288	0.247	0.300	-
32	Lanternfishes	3.31	2.22E-02	3.600	12.000	0.718	0.300	-
33	Leptocephali	2.07	4.00E-02	0.381	1.270	0.200	0.300	-
34	Cephalopods	3.30	1.66E+00	4.000	20.000	0.700	0.200	-
35	Decapods	2.65	1.16E-02	6.000	20.000	0.916	0.300	-
36	Euphausiids	2.42	6.79E-02	22.500	75.000	0.950	0.300	-
37	Mesozooplankton	2.11	2.50E+00	22.000	67.000	0.950	0.328	-
38	Ichthyoplankton	2.50	2.32E+00	15.000	45.000	0.990	0.333	-
39	Gelatinous zooplankton	2.47	8.02E-01	37.000	80.000	0.990	0.463	-
40	Microzooplankton	2.00	1.96E+00	36.000	89.000	0.990	0.404	-
41	Phytoplankton	1.00	2.55E+00	160.000		0.650		
42	Detritus	1.00	5.00E+00			0.993		

“P/B” = Production/Biomass, “Q/B” = Consumption/Biomass, “EE” = Ecotrophic Efficiency, “P/Q” = Production/Consumption, “BA” = Biomass Accumulation

171 Walters et al. (1997) developed Ecosim, a temporal-dynamic model that uses input
172 parameters from a balanced Ecopath model and estimates changes in an ecosystem over time.
173 The dynamics of an Ecosim model are expressed through two differential equations, one that
174 estimates changes in biomass over time, and another that estimates changes in consumption rates
175 at each time step (*sensu* Christensen et al., 2008). During an Ecosim simulation, additional
176 parameters monitor the change in a predator's ability to find and consume prey. The changes in
177 consumption rates are derived from the foraging arena concept (Walters and Juanes, 1993),
178 where prey groups can shift between vulnerable (available to the predator) and invulnerable
179 (unavailable to the predator) states. A high vulnerability parameter signifies top-down control,
180 while a low vulnerability parameter is indicative of bottom-up forcing. Vulnerability parameters
181 were estimated for each functional group using an iterative fitting procedure (Christensen et al.,
182 2008). This procedure tests different vulnerability values for each species and searches for the
183 values that provide the best statistical fit towards a reference time series (Heymans et al., 2016).
184 The vulnerability of larval and juvenile fishes was set at 1 (bottom-up forcing), which
185 significantly improved model performance towards expected adult tuna and billfish trends.

186 *2.3. Parameterization*

187 Information regarding specific sources used to parameterize the model are in Supplementary
188 Material B. Biomass (B ; metric tons km^{-2}) values derive from single-species stock assessments or
189 from fisheries-independent survey data. The finfish stock assessment species that occupy the
190 oceanic GoM have a wider distribution than the model domain. The adult biomass for each
191 multi-stanza group was determined as the quotient of nominal catch in the GoM and exploitation
192 rate that occurs in the model domain ($B = C/F$). Exploitation rate was calculated as the product of
193 the proportion of catches in the GoM relative to the entire stock and the fishing mortality of the

194 entire stock. The data originate from the International Commission for the Conservation of
195 Atlantic Tunas (ICCAT; www.iccat.int/en/). This calculation forces the assumption that
196 standardized catches throughout a stock are a suitable proxy for the distribution of the stock and
197 was chosen in favor of assuming the stock is distributed uniformly across the stock area. Marine
198 mammal and micronekton functional group biomasses were calculated as the product of the
199 standardized abundance (N individuals km⁻²) and mean weight of an organism from either
200 literature values (Trites and Pauly, 1998; NMFS 2019) or survey data. The production/biomass
201 ratio (P/B ; year⁻¹) or total mortality (Z ; year⁻¹) is calculated as the sum of natural mortality and
202 fishing mortality from stock assessments or through empirical relationships (Pauly, 1980;
203 Equation 1):

204 Eq. 1 $M = K^{0.65} * L_{\infty}^{-0.279} * T_c^{0.463}$

205 where M is natural mortality (year⁻¹), K is the curvature parameter from the von Bertalanffy
206 growth equation, L_{∞} is the asymptotic length, and T_c is the mean water temperature in Celsius.

207 Consumption values (Q/B) were estimated based on empirical relationships concerning diet,
208 morphometrics, and water temperature at mean depth (Palomeres and Pauly, 1989; Equation 2):

209 Eq. 2 $\log\left(\frac{Q}{B}\right) = 5.847 + 0.280\log Z - 0.152\log W_{\infty} - 1.360T' + 0.062A + 0.510h + 0.390d$

210 where W_{∞} is the asymptotic weight (g), T' is the mean water temperature expressed as
211 1000/temperature in Kelvins, A is the aspect ratio, and h and d are factors correcting for
212 herbivores and detritivores. The values input into Equation 6 are derived from FishBase (Froese
213 and Pauly, 2019).

214 The diet compositions of all functional groups were estimated from literature values and
215 adjusted to match the requirements of input into an Ecopath model (% weight in diet). To

216 account for uncertainty among input values, each parameter was assigned a rank in EwE's
217 pedigree table, which places a confidence interval around the input value to be used along with
218 resampling techniques. Trophic levels are calculated as fractional values (Odum and Heald,
219 1975) for use in simulation-based analyses. For energy flow related results (i.e., non-Ecosim), a
220 trophic aggregation technique (Ulanowicz, 1995) reorganized functional groups into integer-
221 based trophic levels, as first described in Lindeman (1942).

222

223 One commercial fishing fleet was incorporated: U.S. Pelagic Longline. Landings and fishing
224 effort (No. of hooks) from the longline fleet was obtained from ICCAT databases for the years
225 2011-2018. Bycatch values for the U.S. Pelagic Longline fleet and bycatch mortality rates were
226 gathered from literature sources (Pacheco et al., 2011; Kerstetter and Graves, 2008; Garrison and
227 Stokes, 2014). If bycatch data were not available for a functional group or fishing fleet, all
228 catches were assumed to be landed. The resulting model requires model balancing, a systematic
229 process in which the parameters that were believed to have the greatest uncertainty were adjusted
230 first.

231 *2.4. Time series*

232 The EwE model was developed with the reference year of 2011 and simulated through 2018.
233 The Ecosim model was calibrated to 25 time series of relative changes in catch and biomass
234 values over the eight-year period. Declines in the biomass of five micronekton groups
235 (lanternfishes, bristlemouths, hatchetfishes, decapods, and euphausiids) were forced during
236 simulations (i.e., the user controls the value at each time step; Christensen et al. 2008) according
237 to survey information in 2011 and 2015–2018 (Cook and Sutton, 2017a; Cook and Sutton,
238 2017b; Sutton et al., 2017; Cook and Sutton, 2018; Cook and Sutton, 2020). Time-series biomass

239 values for micronekton groups were calculated as the product of the median standardized
240 abundance and the average weight of an individual of that functional group per sampled year.
241 Only “Gulf Common Water” sampling stations (*sensu* Johnston et al., 2019) were included in
242 micronekton biomass calculations to reduce sample bias caused by the Loop Current. Euphausiid
243 biomass values were estimated at the start of the simulation, so the forced change over time is
244 relative to the initial start value. Dragonfish (Stomiidae) biomass values were not forced during
245 simulations because a significant portion of the population is believed to avoid capture by 10-m²
246 MOCNESS deployments (the standard gear used to catch micronekton in the modelled region;
247 Marks et al., 2020). Due to an absence of reference data, changes in biomass for micronekton
248 functional groups from 2012–2014 are assumed to be a linear function between 2011 and 2015.
249 Interannual changes in the fishing effort for the longline fleet were also forced.

250 2.5. Shifts in trophic structure

251 Using the aforementioned pedigree as a guide for confidence intervals and the original input
252 parameter as a prior value, Monte Carlo simulations (1000 iterations) were run to explore the
253 variation in final output based on original uncertainty (Heymans et al., 2016). Variance among
254 input parameters from the Monte Carlo iterations is displayed in Supplementary Material C.
255 Similar to Choy et al. (2016), feeding guilds were established for all functional groups with a
256 trophic level greater than 3.5 to differentiate among feeding of top predators. A trophic level of
257 3.5 was chosen as a cut-off because this group contains adult cohorts of tunas and billfishes,
258 micronektivorous fishes, and marine mammals. We employed this method for both 2011 (start of
259 simulation) and 2018 (end of simulation) to identify trophic shifts among top predators in the
260 ecosystem. The average diet matrix (mean of 1000 iterations) for each year was calculated. A
261 hierarchical clustering method performed on a Bray-Curtis similarity matrix determined the

262 feeding guilds in each year using 60% similarity as a cut-off (Clarke and Gorley, 2006). These
263 guilds were overlaid with fitted eigen vectors on an MDS plot to aid in the interpretation of
264 clustering results. All multivariate analyses were conducted using the R vegan package (Oksanen
265 et al., 2019).

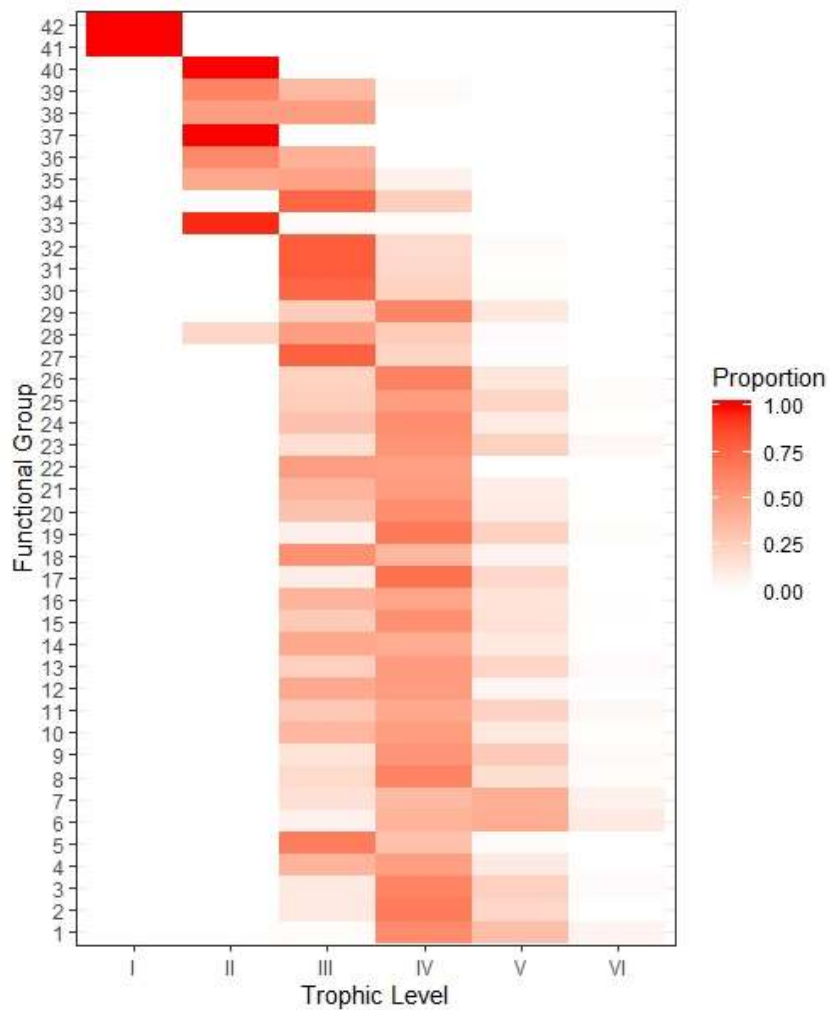
266 The mixed trophic impact (MTI) was calculated (Ulanowicz and Puccia, 1990) individually
267 for each iteration, for each functional group pair in the model ($N = 1849$), and for each year ($n =$
268 8). Averages and standard deviations were calculated for every functional group pair every year,
269 treating the iterations as replicates. For each pair, a linear model was developed to examine
270 whether the trend in MTI was a significant change or not. A p-value of less than 0.05 was
271 considered statistically significant. The code used to calculate the MTI from the Monte Carlo
272 model output is available as an R Markdown document on GitHub
273 (www.github.com/mwood078-oGom-EwE).

274 3. Results

275 *3.1. Ecopath results*

276 The model comprises approximately five trophic levels, with sharks, marine mammals, and
277 adult tunas and billfishes occupying the top of the food web. The micronekton groups that were
278 forced in this simulation occupied trophic levels ranging from 2.42 to 3.33. A decomposition of
279 the origin of flows by integer-based trophic level for each functional group revealed that for all
280 mesopelagic zooplanktivorous fish functional groups, greater than 75% of the energy they
281 receive placed them in the third trophic level (Figure 2). The two primary producer groups
282 (including detritus) accounted for 29.1% of the total standing stock biomass in the system, while
283 upper trophic level organisms ($TL > 4$) amounted to just 10.1% of the total biomass. The largest
284 proportion of biomass was zooplankton ($TL = 2$), which accounted for 35.9% of the total

285 biomass in the system. Zooplankton was responsible for 38.4% of the total system throughput
286 (sum of consumption by predators, export, flow to detritus, and respiration), while upper trophic
287 level organisms were only responsible for 3.7% of the total throughput. Detritus was the origin
288 of a significant proportion of the total flow through the system (36%), which can be a sign of a
289 mature ecosystem (Odum and Heald, 1975) and highlights the importance of detritus in the
290 oceanic GoM.



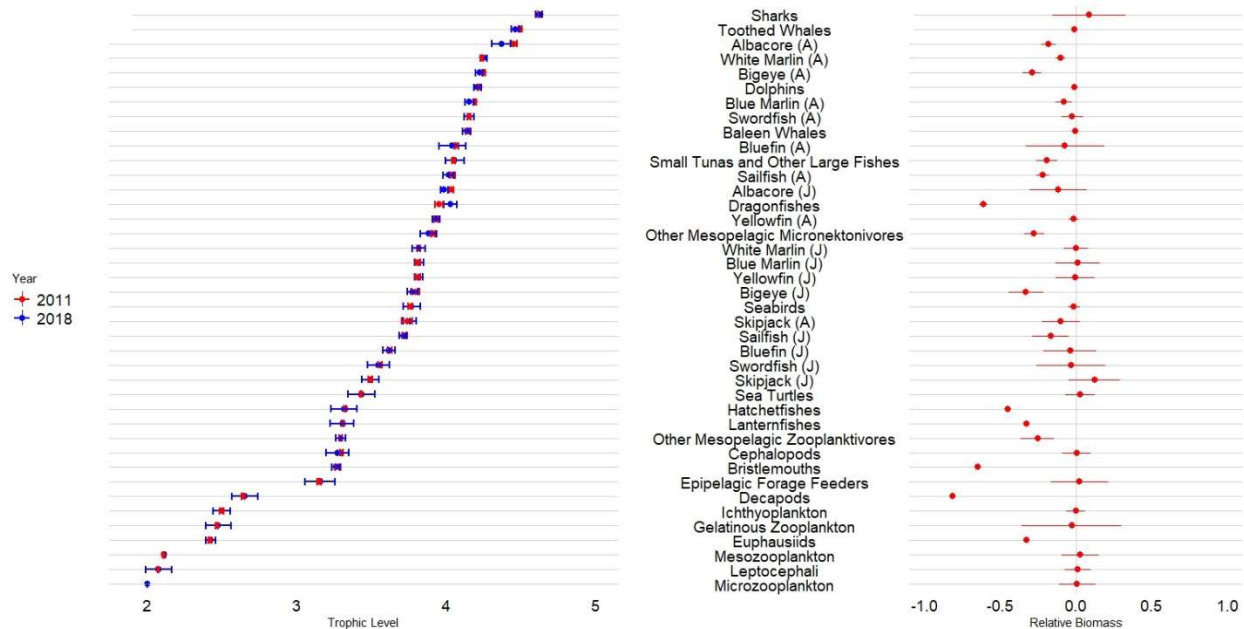
291
292 **Figure 2.** Shade plot of the trophic level decomposition for each functional group based on diet
293 composition. Red values are positive, shaded to proportion. Functional groups with positive

294 values in multiple trophic levels indicate feeding on a variety of trophic levels (i.e., omnivory).
295 Weighted averages equate to the mean trophic level of the functional group in Table 1.

296

297 *3.2. Simulated processes*

298 Throughout the eight-year simulation, all functional groups experienced some change in their
299 biomass and trophic level, but many changes were discrete (Figure 3). Thirty-one of the 42
300 functional groups within the model showed a decrease in biomass throughout the simulation. The
301 three functional groups that benefited the most throughout the simulation were juvenile skipjack
302 (13.18% increase), oceanic sharks (7.79% increase), and mesozooplankton (3.01% increase). The
303 most negatively affected functional groups in terms of percentage change were decapod
304 crustaceans (81.10% decrease), bristlemouths (65.2% decrease), and dragonfishes (61.5%
305 decrease). Twenty-five functional groups experienced a decrease in trophic level throughout the
306 simulation. The largest overall changes in trophic level (TL) occurred in fishes that rely heavily
307 on mesopelagic micronekton as a prey source: adult albacore tuna (0.08 TL decrease), juvenile
308 albacore tuna (0.08 TL decrease), and dragonfishes (0.04 TL increase). In general, 19 functional
309 groups decreased in both trophic level and biomass, while just eight increased in both (Figure 3).



310

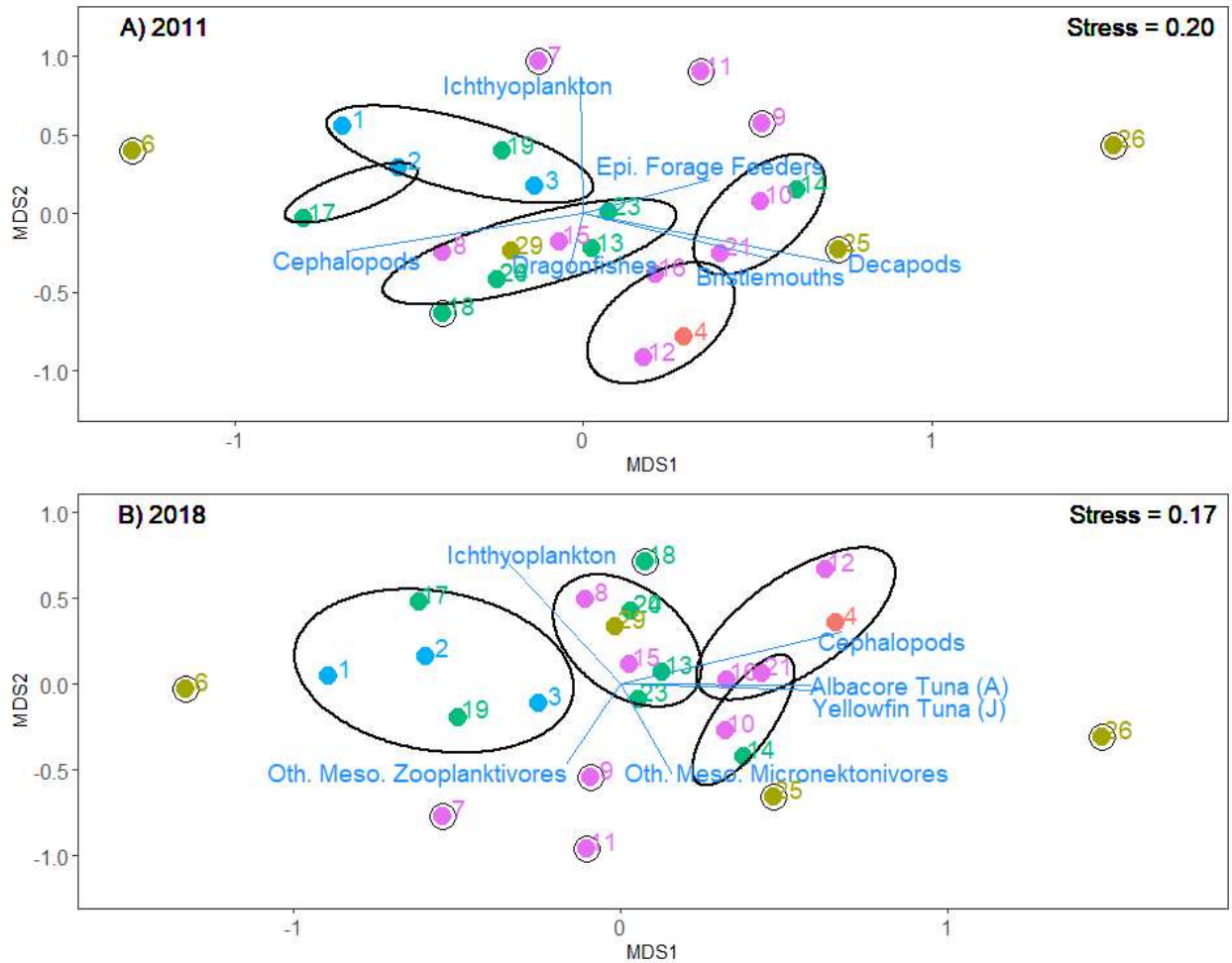
311 **Figure 3.** Trophic level and biomass changes between 2011 and 2018. Functional groups are
 312 ordered by trophic level. “A” and “J” correspond to “adult” and “juvenile” as determined by the
 313 age of maturity. Error bars are 95% confidence intervals originating from 1000 model iterations.
 314 A) Mean trophic level by functional group for 2011 (red) and 2018 (blue). B) Relative biomass
 315 calculated as: (final – initial) / initial.

316

317 *3.3. Shifts in diet*

318 The underlying mechanics behind an Ecopath with Ecosim model rely on the predator-prey
 319 relationships driven by the diet matrix. Any change in the trophic structure that is not captured
 320 by changes in the trophic level of a functional group should be reflected in the diet matrix as a
 321 significant shift in prey taxa consumed (% biomass) relative to other predators at a similar
 322 trophic level. To target the effect of declines in micronekton biomass, two sets of feeding guilds
 323 were established for functional groups with a trophic level greater than 3.5. In 2011, 12 feeding
 324 guilds were established based on the similarity of diets (Figure 4a). Predation on bristlemouths,

325 decapod crustaceans, epipelagic forage feeders, cephalopods, ichthyoplankton, and dragonfishes
326 best explained the food web structure. Lanternfishes are notably absent from this list because
327 they are eaten by nearly all upper trophic level organisms, and do not contribute to diverging
328 diets. Although marine mammals consume mesopelagic prey, their diets were separated from
329 many tuna and billfish species because of an affinity for cephalopods and larval fishes (Figure
330 4a). Seven single-group feeding guilds were present: oceanic sharks, adult albacore tuna, adult
331 bigeye tuna, adult bluefin tuna, adult white marlin, small tunas and other large predators, and
332 dragonfishes. An epipelagic-fish feeding guild was composed of seabirds, juvenile bluefin tuna,
333 and juvenile yellowfin tuna. Dragonfishes were a bit of an outlier among the other functional
334 groups, as their diet composition is primarily mesopelagic zooplanktivores. Other diets are more
335 diverse than dragonfishes, including cephalopods and micronektonivores, so the dragonfish
336 placement in this plot was more indicative of a vastly different diet compared to other top
337 predators in the ecosystem.



338

339 **Figure 4.** Ordination plots of the upper trophic level organisms (TL > 3.5) according to Bray-
 340 Curtis similarity matrices. Guilds are displayed by ellipses. The prey groups that explained the
 341 majority of the matrix structure are shown as blue vectors and labeling. Predator groups are
 342 distinguished by taxon: blue = marine mammals, red = seabirds, purple = tunas; green =
 343 billfishes; yellow = other fishes.

344

345 In 2018, eleven feeding guilds were recognized, and some functional groups have
 346 transitioned to have similar diets to other functional groups (i.e., changed feeding guild; Figure
 347 4b). Decapod crustaceans, bristlemouths, and dragonfishes no longer explained the majority of

348 the food web structure, and instead were replaced by adult albacore tuna, juvenile yellowfin tuna,
349 and other mesopelagic fishes. Compared to 2011, other upper trophic level organisms explained
350 more of the food web structure than mesopelagics, which can be interpreted as a reduction in the
351 mesopelagic biomass constricting the diversity of prey available to top predators.

352 *3.4. Mixed trophic impact analysis*

353 Individual linear models (n = 1849) indicated that there was a change in 27.3% of the
354 functional group interactions during this simulation (Figure 5). Although each functional group
355 acted as both the impacting and impacted group towards each other functional group in the
356 model, a change in one end of the interaction was reciprocated with a change in the other side of
357 the relationship 47 times, which is likely an indication ecosystem complexity. Of the interactions
358 where there was a direct trophic relationship (i.e., predator-prey interaction; n = 505), 32.3% of
359 the interactions showed a change from 2011-2018 (Table 2). An uneven number of direct top-
360 down and bottom-up interactions was the result of cyclical relationships (e.g., “cannibalism”).
361 During the simulation, direct relationships strengthened more frequently than they weakened for
362 both top-down and bottom-up interactions (Table 2). Contrary to direct interactions, indirect
363 interactions weakened more frequently than strengthened (Table 2). Indirect interactions were
364 the most common type of relationship (n = 1344) and changed less frequently than direct
365 interactions (24.7% frequency). Direct top-down interactions changed more than the other three
366 types of interactions, suggesting these types of relationships are more labile in the oceanic GoM.

367

368

369 **Table 2.** Contingency table of the number of functional group interactions that showed a change
 370 throughout the time series. The total number of interactions is in parentheses.

Interaction	Strengthened	Weakened	Unchanged
Direct Top-Down (318)	30.82%	18.87%	50.31%
Direct Bottom-Up (323)	8.98%	6.19%	84.83%
Indirect Top-Down (618)	9.71%	12.62%	77.67%
Indirect Bottom-Up (590)	5.42%	21.69%	72.88%

371



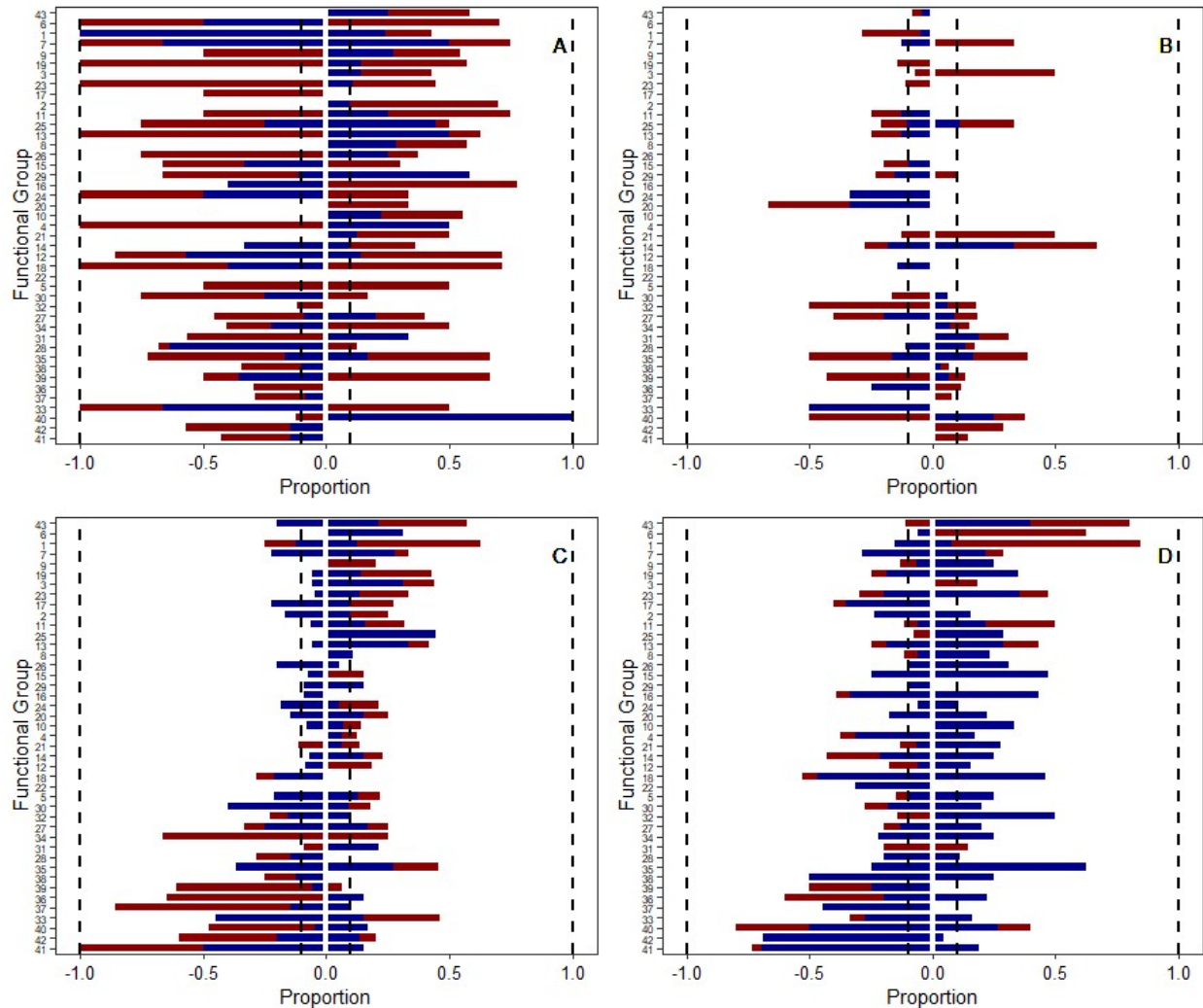
372

373 **Figure 5.** Matrix of the trend observed in all functional group pairs over time. The background
 374 colors represent the initial role that functional group serves in the interaction: dark blue = prey
 375 (bottom-up), dark red = predator (top-down), light blue = indirect bottom-up, light red = indirect
 376 top-down. Lines represent the trend in the interaction over time: flat = no change, increasing =

377 strengthened, decreasing = weakened. Numbers correspond to functional groups in Table 1. F1
378 corresponds to the U.S. Pelagic Longline fishing fleet.

379

380 When organizing groups by trophic level, there was no apparent trend in the proportion of
381 changed interactions related to a functional group role in the ecosystem (Figure 6). The changes
382 seen in direct interactions were focused on certain functional groups, as opposed to being shared
383 across all groups in the system (i.e., some functional groups had zero interactions change, while
384 others had many). Changes among direct top-down interactions were more frequent than among
385 direct bottom-up interactions (Figure 6). Both types of indirect interactions (top-down and
386 bottom-up) changed in small proportions for all functional groups in the model, suggesting that
387 the entire ecosystem experienced some change between 2011 and 2018. The preponderance of
388 weakening indirect interactions (and scarcity of strengthening) suggests ecosystem resiliency has
389 decreased (Bertness et al., 2015), as future ecosystem processes will now be more driven by
390 direct interactions.



391
 392 **Figure 6.** Stacked barplots showing the proportion of interactions that changed for each
 393 functional group between 2011 and 2018. Values to the right of 0 represent the functional group
 394 acting as the impacting group, and values to the left of 0 are when the group is the impacted
 395 group. Total bar height is the overall proportion of changed interactions (0-1). Colors represent
 396 the directionality of change, where red indicates interactions that strengthened and blue indicates
 397 interactions that weakened. Vertical black lines mark 10 and 100% of interactions for readability.
 398 Functional groups are organized in descending order by trophic level, beginning with the fishery
 399 (Functional group 43). A) Direct top-down interactions, B) direct bottom-up interactions, C)
 400 indirect top-down interactions, and D) indirect bottom-up interactions.

401

402 4. Discussion

403 The role of mesopelagic micronekton as ‘wasp-waist’ controllers in pelagic ecosystems is
404 well documented (Griffiths et al., 2013; Choy et al., 2016). Compared to neritic habitats, pelagic
405 organisms have less specific diets, but preferential preys exist (Drazen and Sutton, 2017). The
406 feeding guilds that mesopelagic fishes can occupy are limited because the concentration of
407 particulates in the water column is too low for filter feeding at mesopelagic depths (Herring,
408 2002), and herbivory is rare (Robison, 1984). Thus, carnivory dominates the feeding mode of
409 mesopelagic fishes. Just three of the direct top-down interactions that involve myctophids,
410 sternoptychids, gonostomatids, and other mesopelagic zooplanktivores as predators strengthened
411 throughout the simulation, while seven weakened (all from the aggregate group). A dearth of
412 change among these functional groups, which had significant declines in biomass, is evidence of
413 a poor ability to switch prey among a diminished prey field. These restricted diet options,
414 combined with declines in macrozooplankton populations, will likely inhibit the recovery of
415 micronekton fish populations as food is less prevalent. Furthermore, the direct top-down
416 interactions exerted on the mesopelagic zooplanktivorous fish groups strengthened in 23 of 60
417 possible interactions and weakened in only five. Decreased mesopelagic zooplanktivorous fish
418 populations in the oceanic GoM should hypothetically be relieved of predation pressure
419 (regardless of where the population was pre-2011), but in many instances, the role they provide
420 as prey has become more intense. Similar to the euphausiid-capelin (*Mallotus villosus*) trophic
421 relationship in Newfoundland waters (Obradovich et al., 2014), a persistent decline in
422 micronekton populations may have inauspicious effects on predator population growth.

423 Zooplankton populations are pivotal to the stability of oceanic ecosystems, as they are the
424 food-web link between autotrophic organisms and secondary consumers. Filter-feeding

425 zooplankton package pico- (10^{-12} m) and nano-size particles (10^{-9} m) into a consumable material
426 for other consumers. Others, such as decapod crustaceans and some euphausiids, consume
427 microzooplankton and mesozooplankton, occasionally competing with small fishes (Heffernan
428 and Hopkins, 1981; Kinsey and Hopkins, 1994; Hopkins and Sutton, 1998). This wide niche
429 breadth throughout the trophic level is why approximately two-fifths of the total system
430 throughput occurs at the zooplankton trophic level. Similar to fishes, the direct interactions
431 involving zooplankton were labile. Therefore, pelagic zooplankton was predicted to experience
432 greater predation pressure in 2018 despite their population decline. However, an
433 underrepresented portion of many food-web models is the role of gelatinous zooplankton in the
434 transfer of energy through the ecosystem. Although this model incorporates occurrences of
435 gelatinous feeding by upper trophic level organisms (Cardona et al., 2012), these values are
436 believed to be heavily underreported in the literature (Drazen and Sutton, 2017). The stability of
437 the oceanic GoM ecosystem is dependent on the stability of the zooplankton trophic level, so it is
438 imperative to understand the interactions that control their population dynamics.

439 Approximately one-quarter of all possible trophic interactions in the oceanic GoM changed
440 between 2011 and 2018. For each functional group pair, i and j , there are two types of
441 interactions. One interaction is where group i is the group exerting impact on group j , and
442 another is where group i is receiving the impact from group j . In an ecosystem with high
443 modularity (i.e., several guilds of organisms only interact with each other), a change in the top-
444 down impact of one group to another should result in a change of the bottom-up impact in the
445 reciprocating interaction, as a result of ecosystem simplicity. However, in this exercise, a change
446 in the interaction between two groups did not often result in a change in the opposite direction.
447 For example, the direct top-down pressure that dragonfishes exert on hatchetfishes weakened,

448 but the direct bottom-up support hatchetfishes provide to dragonfishes did not change from
449 2011–2018. This phenomenon is likely attributable to the complexity of the oceanic GoM
450 micronekton assemblage (Hopkins and Lancraft 1984) that allows upper trophic level predators
451 to shift their diet to new preys rather than starve. The importance of mesopelagic micronekton in
452 the diet of apex predators in the oceanic zone suggests that changes in population sizes within the
453 micronekton community could have a direct impact on the predatory success of these apex
454 predators (Duffy et al., 2017), as this exercise shows. Declined predator success will result in
455 declined biomass, but GoM-specific abundance indices suggest that yellowfin and bluefin tuna
456 populations may be relatively stable or increasing (Anon, 2017; Anon, 2019). The potential
457 underestimates in apex predator biomass is likely a product of an inability to model an “open-
458 system” where organisms could leave but suggests that the results related to the top-down
459 pressure on micronekton may be conservative. In reality, opportunistic predation and long-
460 distance migrations by apex predators likely provide a buffer towards the stability of these
461 predator populations (Ménard et al., 2006), despite declines in major prey resources in the GoM.
462 These diet shifts were reflected in the calculation of the MTI as the declined prey group was
463 predicted to experience less predation pressure from the predator, and the predator now benefits
464 less from the existence of the former prey group (lower diet contribution). In stable ecosystems,
465 individual populations can fluctuate because species that occupy a similar niche can replace
466 declining populations (Holling, 1973). In the context of this exercise, changes among top-down
467 and bottom-up effects may not reflect permanent changes to the trophic structure of the
468 ecosystem, but instead, a temporary change based on fluctuations in prey abundances. However,
469 simulated biomass declines in other micronekton groups (e.g., dragonfishes, cephalopods, and

470 other mesopelagic micronektivorous fishes) indicates the northern GoM may no longer be a
471 plentiful foraging ground for upper trophic level organisms compared to 2011.

472 Changes in the MTI of one functional group on another will mostly be influenced by changes
473 in diet and biomass. Significant changes in diet (relative to the rest of the ecosystem) should
474 adjust the trophic level of a functional group throughout a simulation, and diet is influenced by
475 shifts in the biomass of prey groups over time (Shannon et al., 2014). Declines in several
476 micronekton groups in this model led to a slight increase in the biomass of groups of a similar
477 niche that were not forced (e.g., mesozooplankton), but to a decline in those dependent on
478 mesopelagic micronekton as a prey resource (e.g., dragonfishes). An investigation of the MTI
479 over time provides a more refined view into potential shifts in the role of each organism relative
480 to others within the system and could be used to assess other oceanic ecosystems.

481 The total effort of fishers on an annual basis is a dynamic process influenced by the
482 availability of target fishes, length of the fishing season, and unexpected shutdowns (Monroy et
483 al., 2010). In an ecosystem model, the role of each fishing fleet is to remove biomass (similar to
484 an apex predator). Fluctuations in the effort of a fishing fleet influence the amount of fishing
485 pressure exerted on each commercial species. Since 2011, the fishing effort by the U.S. Pelagic
486 Longline Fleet in the GoM has declined as a response to fishing regulations implemented in the
487 region to reduce bluefin tuna bycatch (NMFS, 2020). This decline in the fishing effort has
488 lessened the fishing mortality exerted on commercial groups, having a negative indirect effect on
489 many intermediate trophic level groups. Micronekton interact on a much smaller spatial scale
490 than large pelagic fishes but exist in large numbers as a well-dispersed assemblage (Milligan and
491 Sutton, 2020). Still, the commercial impact of declines in mesopelagic micronekton in the GoM
492 is untested. Future addenda to management and conservation policies in the oceanic GoM should

493 be cognizant of declined prey abundances that could influence the direct trophic relationships
494 with species of economic concern and energy flows throughout the ecosystem.

495 The 2010 *Deepwater Horizon* oil spill likely had an immediate negative impact on oceanic
496 biota (Abbriano et al., 2011), but intense data collection regimes began after the disturbance
497 (Sutton et al., 2020). Without a pre-disturbance reference point, it is difficult to discern between
498 natural changes and human-influenced changes. Therefore, this exercise does not imply that
499 anthropogenic impacts are responsible for changes within the ecosystem. Instead, these results
500 may provide an example of the dynamic nature of complex ecosystems with opportunistic apex
501 predators and diverse intermediate trophic level communities.

502 5. Acknowledgements

503 This research was made possible in part by a grant from The Gulf of Mexico Research
504 Initiative and in part by a grant from the NOAA RESTORE Science Program. Data are publicly
505 available through the Gulf of Mexico Research Initiative Information & Data Cooperative
506 (GRIIDC) at <https://data.gulfresearchinitiative.org> (doi: 10.7266/N7VX0DK2;
507 10.7266/N70P0X3T; 10.7266/N7XP7385; 10.7266/N7902234; 10.7266/n7-ac8e-0240). This is
508 contribution #233 from the Center for Coastal Oceans Research in the Institute of Water and
509 Environment at Florida International University. We are grateful for Rosanna Milligan, April
510 Cook, Walt Ingram, and Skyler Sagarese for their discussions about parameterization of this
511 model. The authors are thankful to an anonymous reviewer for helpful comments on the
512 manuscript. All authors declare no conflict of interest.

513 6. Literature Cited

514 Abbriano, R. M., M. M. Carranza, S. L. Hogle, R. A. Levin, A. N. Netburn, K. L. Seto, S. M.
515 Snyder, and P.J.S. Franks. 2011. Deepwater Horizon oil spill: A review of the planktonic
516 response. *Oceanogr.* 24: 294–301. <http://dx.doi.org/10.5670/oceanog.2011.80>.

517 Ainsworth, C. H., M. J. Schirripa, and H. N. Morzaria-Luna. 2015. An Atlantis ecosystem model
518 for the Gulf of Mexico supporting integrated ecosystem assessment. NOAA Technical
519 Memorandum. NMFS-SEFSC-676. <http://doi.org/10.7289/V5X63JVH>

520 Anon. 2017. Report of the 2017 ICCAT Bluefin Stock Assessment Meeting. Madrid, Spain.
521 www.iccat.int. Last Accessed 04/13/2020.

522 Anon. 2019. Report of the 2019 ICCAT Yellowfin Tuna Stock Assessment Meeting. Grand-
523 Bassam, Cote d’Ivoire. www.iccat.int. Accessed 04/13/2020.

524 Bertness, M. D., C. P. Brisson, and S. M. Crotty. 2015. Indirect human impacts turn off
525 reciprocal feedbacks and decrease ecosystem resilience. *Oecologia.* 178: 231–237.
526 <https://doi.org/10.1007/s00442-014-3166-5>

527 Cardona, L., I. A. De Quevedo, A. Borrell, and A. Aguilar. 2012. Massive consumption of
528 gelatinous plankton by Mediterranean apex predators. *PloS one.* 7: e31329.
529 <https://doi.org/10.1371/journal.pone.0031329>

530 Chagaris, D. D., B. Mahmoudi, C. J. Walters, and M. S. Allen. 2015. Simulating the trophic
531 impacts of fishery policy options on the West Florida Shelf using Ecopath with Ecosim. *Mar.*
532 *Coastal Fish.* 7: 44–58. <https://doi.org/10.1080/19425120.2014.966216>

533 Choy, C. A., B. N. Popp, C. C. S. Hannides, and J. C. Drazen. 2016. Trophic structure and food
534 resources of epipelagic and mesopelagic fishes in the North Pacific Subtropical Gyre
535 ecosystem inferred from nitrogen isotopic compositions. *Limnol. Oceanogr.* 60: 1156–1171.
536 <https://doi.org/10.1002/lno.10085>

537 Christensen, V., C. J. Walters, D. Pauly, and R. Forrest. 2008. Ecopath with Ecosim version 6: a
538 User's guide, November 2008 edition. Vancouver, Canada: University of British Columbia
539 Fisheries Centre.

540 Clarke, K. R., and R. N. Gorley. 2006. PRIMER V6: user manual and tutorial. Primer-E,
541 Plymouth, UK

542 Coll, M., N. Bahamon, F. Sardá, I. Palomera, S. Tudela, P. Suuronen. 2008. Improved trawl
543 selectivity: effects on the ecosystem in the South Catalan Sea (NW Mediterranean). *Mar.*
544 *Ecol. Prog. Ser.* 355: 131–147. <https://doi.org/10.3354/meps07183>

545 Coll, M., and J. Steenbeek. 2017. Standardized ecological indicators to assess aquatic food webs:
546 The ECOIND software plug-in for Ecopath with Ecosim models. *Environ. Modell. Software.*
547 89: 120–130. <https://doi.org/10.1016/j.envsoft.2016.12.004>

548 Cook, A., and T. T. Sutton. 2017a. Inventory of Gulf oceanic fauna data including species,
549 weight, and measurements. Cruises DP01 May 1-8, 2015 and DP02 August 9-21, 2015 R/V
550 on the *Point Sur* in the Northern Gulf of Mexico. Distributed by: Gulf of Mexico Research
551 Initiative Information and Data Cooperative (GRIIDC), Harte Research Institute, Texas
552 A&M University-Corpus Christi. <https://doi.org/10.7266/N70P0X3T>

553 Cook, A., and T. T. Sutton. 2017b. Inventory of Gulf of Mexico oceanic fauna data including
554 species, weight, and measurements from R/V *Point Sur* (Cruises DP03 and DP04) May-
555 August, 2016. Distributed by: Gulf of Mexico Research Initiative Information and Data
556 Cooperative (GRIIDC), Harte Research Institute, Texas A&M University-Corpus Christi.
557 <https://doi.org/10.7266/N7XP7385>

558 Cook, A., and T. T. Sutton. 2018. Inventory of oceanic fauna data including species, weight, and
559 measurements from R/V *Point Sur* (Cruise DP05) in the Gulf of Mexico from 2017-05-01 to
560 2017-05-11. Distributed by: Gulf of Mexico Research Initiative Information and Data
561 Cooperative (GRIIDC), Harte Research Institute, Texas A&M University-Corpus Christi.
562 <https://doi.org/10.7266/N7902234>

563 Cook, A., and T. T. Sutton 2020. Inventory of oceanic fauna data including species, weight, and
564 measurements from R/V *Point Sur* cruise PS19-04 (DP06) in the Gulf of Mexico from 2018-
565 07-19 to 2018-08-01. Distributed by: Gulf of Mexico Research Initiative Information and
566 Data Cooperative (GRIIDC), Harte Research Institute, Texas A&M University-Corpus
567 Christi. <https://doi.org/10.7266/n7-ac8e-0240>

568 Costanza, R. and M. Mageau, M. 1999. What is a healthy ecosystem?. *Aquat. Ecol.* 33: 105–115.
569 <https://doi.org/10.1023/A:1009930313242>

570 de Mutsert, K., J. H. Cowan Jr., and C. J. Walters. 2012. Using Ecopath with Ecosim to explore
571 nekton community response to freshwater diversion into a Louisiana estuary. *Mar. Coastal*
572 *Fish.* 4: 104–116. <https://doi.org/10.1080/19425120.2012.672366>

573 de Mutsert, K., J. Steenbeek., K. Lewis, J. Buszowski, J. H. Cowan Jr., and V. Christensen.
574 2016. Exploring effects of hypoxia on fish and fisheries in the northern Gulf of Mexico using
575 a dynamic spatially explicit ecosystem model. *Ecol. Modell.* 331: 142–150.
576 <https://doi.org/10.1016/j.ecolmodel.2015.10.013>

577 Drazen, J. C., and T. T. Sutton. 2017. Dining in the Deep: The Feeding Ecology of Deep-Sea
578 Fishes. *Annu. Rev. Mar. Sci.* 9: 337–366. [https://doi.org/10.1146/annurev-marine-010816-](https://doi.org/10.1146/annurev-marine-010816-060543)
579 [060543](https://doi.org/10.1146/annurev-marine-010816-060543)

580 Duffy, L. M., P. M. Kuhnert, H. R. Pethybridge, J. W. Young, R. J. Olson, J. M. Logan, N. Goñi,
581 E. Romanov, V. Allain, M. D. Staudinger, M. Abecassis, C. A. Choy, A. J. Hobday, M.
582 Simier, F. Galván-Magaña, M. Potier, and F. Ménard. 2017. Global trophic ecology of
583 yellowfin, bigeye, and albacore tunas: Understanding predation on micronekton communities
584 at ocean-basin scales. *Deep Sea Res., Part II.* 140: 55–73.
585 <https://doi.org/10.1016/j.dsr2.2017.03.003>

586 Fromentin, J. M., and J. E. Powers. 2005. Atlantic bluefin tuna: population dynamics, ecology,
587 fisheries and management. *Fish Fish.* 6: 281–306. [https://doi.org/10.1111/j.1467-](https://doi.org/10.1111/j.1467-2979.2005.00197.x)
588 [2979.2005.00197.x](https://doi.org/10.1111/j.1467-2979.2005.00197.x)

589 Froese, R., and D. Pauly. Editors. 2019. FishBase. World Wide Web electronic publication.
590 www.fishbase.org, version (12/2019).

591 Frost, B. W., and L. E. McCrone. 1978. Vertical distribution, diel vertical migration, and
592 abundance of some mesopelagic fishes. *Fish. Bull.* 76: 751–770.

593 Garrison, L. P., and L. Stokes. 2014. Estimated bycatch of marine mammals and sea turtles in the
594 US Atlantic pelagic longline fleet during 2013. NOAA technical memorandum NMFS-
595 SEFSC-672. <https://doi.org/10.7289/V50C4SQB>

596 Geers, T. M., E. K. Pikitch, and M. G. Frisk. 2016. An original model of the northern Gulf of
597 Mexico using Ecopath with Ecosim and its implications for the effects of fishing on
598 ecosystem structure and maturity. *Deep Sea Res., Part II.* 129: 319–331.
599 <https://doi.org/10.1016/j.dsr2.2014.01.009>

600 Griffiths, S. P., R. J. Olson, and G. M. Watters. 2013. Complex wasp-waist regulation of pelagic
601 ecosystems in the Pacific Ocean. *Rev. Fish Biol. Fish.* 23: 459–475.
602 <https://doi.org/10.1007/s11160-012-9301-7>

603 Grüss, A., E. A. Babcock, S. R. Sagarese, M. Drexler, D. D. Chagaris, C. H. Ainsworth, B.
604 Penta, S. Derada, and T. T. Sutton. 2016. Improving the spatial allocation of functional group
605 biomasses in spatially-explicit ecosystem models: insights from three Gulf of Mexico
606 models. *Bull. Mar. Sci.* 92: 473–496. <https://doi.org/10.5343/bms.2016.1057>

607 Guinotte, J. M., and V. J. Fabry. 2008. Ocean acidification and its potential effects on marine
608 ecosystems. *Ann. N. Y. Acad. Sci.* 1134: 320–342. <https://doi.org/10.1196/annals.1439.013>.

609 Heffernan, J. J., and T. L. Hopkins. 1981. Vertical distribution and feeding of the shrimp genera
610 *Gennadas* and *Bentheogennema* (Decapoda: Penaeidea) in the eastern Gulf of Mexico. *J.*
611 *Crustacean Biol.* 1: 461–473. <https://doi.org/10.2307/1548124>

612 Herring, P. 2002. *The biology of the deep ocean.* Oxford University Press.

613 Heymans, J. J., M. Coll, J. S. Link, S. Mackinson, J. Steenbeek, C. Walters, and V. Christensen.
614 2016. Best practice in Ecopath with Ecosim food-web models for ecosystem-based
615 management. *Ecol. Modell.* 331: 173–184. <https://doi.org/10.1016/j.ecolmodel.2015.12.007>

616 Hilborn, R., 2011. *Overfishing: What Everyone Needs to Know*. Oxford University Press.

617 Hoegh-Guldberg, O., and J. F. Bruno. 2010. The impact of climate change on the world's marine
618 ecosystems. *Sci.* 328: 1523–1528. <https://doi.org/10.1126/science.1189930>

619 Holling, C. S. 1973. Resilience and stability of ecological systems. *Annual review of ecology
620 and systematics.* 4: 1–23. <https://doi.org/10.1146/annurev.es.04.110173.000245>

621 Hopkins T. L., and T. M. Lancraft. 1984. The composition and standing stock of mesopelagic
622 micronekton at 27° N 86° W in the eastern Gulf of Mexico. *Contr. Mar. Sci.* 27: 143–158.

623 Hopkins, T. L., and T. T. Sutton. 1998. Midwater fishes and shrimps as competitors and resource
624 partitioning in low latitude oligotrophic ecosystems. *Mar. Ecol. Prog. Ser.* 164: 37–45.
625 <https://doi.org.10.3354/meps164037>

626 Hopkins, T. L., T. T. Sutton, and T. M. Lancraft. 1996. The trophic structure and predation
627 impact of a low latitude midwater fish assemblage. *Prog. Oceanogr.* 38: 205–239.
628 [https://doi.org/10.1016/S0079-6611\(97\)00003-7](https://doi.org/10.1016/S0079-6611(97)00003-7)

629 Johnston, M. W., R. J. Milligan, C. G. Easson, S. deRada, D. C. English, B. Penta, and T. T.
630 Sutton. 2019. An empirically validated method for characterizing pelagic habitats in the
631 Gulf of Mexico using ocean model data. *Limnol. Oceanogr.: Methods.* 17: lom3.10319.
632 <https://doi.org/10.1002/lom3.10319>

633 Kerstetter, D. W., and J. E. Graves. 2008. Postrelease Survival of Sailfish Caught by Commercial
634 Pelagic Longline Gear in the Southern Gulf of Mexico. *North Am. J. Fish. Manage.* 28:
635 1578–1586. <https://doi.org/10.1577/M07-202.1>

636 Kinsey, S. T. and T. L. Hopkins, 1994. Trophic strategies of euphausiids in a low-latitude
637 ecosystem. *Mar. Biol.* 118: 651–661. <https://doi.org/10.1007/BF00347513>

638 Lerner, J. D., D. W. Kerstetter, E. D. Prince, L. Talaue-McManus, E. S. Orbesen, A. Mariano, D.
639 Snodgrass, and G. L. Thomas. 2013. Swordfish vertical distribution and habitat use in
640 relation to diel and lunar cycles in the western North Atlantic. *Tran. Am. Fish. Soc.* 142: 95–
641 104. <https://doi.org/10.1080/00028487.2012.720629>

642 Levin, P. S., M. J. Fogarty, G. C. Matlock, and M. Ernst. 2008. Integrated ecosystem
643 assessments. NOAA Technical Memorandum. NMFS-NWFSC-92. Available at:
644 <https://swfsc.noaa.gov/publications/FED/01272.pdf>.

645 Libralato, S., V. Christensen, V. and D. Pauly. 2006. A method for identifying keystone species
646 in food web models. *Ecol. Modell.* 195: 153–171.
647 <https://doi.org/10.1016/j.ecolmodel.2005.11.029>

648 Lindeman, R. L. 1942. The Trophic-Dynamic Aspect of Ecology. *Ecol.* 23: 399–417.
649 <https://doi.org/10.2307/1930126>

650 Marks, A. D., D. W. Kerstetter, D. M. Wyanski, and T. T. Sutton. 2020. Reproductive Ecology
651 of Dragonfishes (Stomiiformes: Stomiidae) in the Gulf of Mexico. *Front. Mar. Sci.* 7: 1–17.
652 <https://doi.org/10.3389/fmars.2020.00101>

653 Ménard, F., C. Labrune, Y. J. Shin, A. S. Asine, and F. X. Bard. 2006. Opportunistic predation in
654 tuna: a size-based approach. *Mar. Ecol. Prog. Ser.* 323: 223–231.
655 <https://doi.org/10.3354/meps323223>

656 Milligan, R. J., and T. T. Sutton. 2020. Dispersion Overrides Environmental Variability as a
657 Primary Driver of the Horizontal Assemblage Structure of the Mesopelagic Fish Family
658 Myctophidae in the Northern Gulf of Mexico. *Front. Mar. Sci.* 7: 1–13.
659 <https://doi.org/10.3389/fmars.2020.00015>

660 Monaco, M. E., and R. E. Ulanowicz. 1997. Comparative ecosystem trophic structure of three
661 US mid-Atlantic estuaries. *Mar. Ecol. Prog. Ser.* 161: 239–254.
662 <https://doi.org/10.3354/meps161239>

663 Monroy, C., S. Salas, and J. Bello-Pineda. 2010. Dynamics of fishing gear and spatial allocation
664 of fishing effort in a multispecies fleet. *North Am. J. Fish. Manage.* 30: 1187–1202.
665 <https://doi.org/10.1577/M09-101.1>

666 National Marine Fisheries Service (NMFS). 2019. US Atlantic and Gulf of Mexico Marine
667 Mammal Stock Assessments – 2019. NOAA Technical Memorandum NMFS-NE-264.
668 Available at: [https://www.fisheries.noaa.gov/national/marine-mammal-protection/marine-](https://www.fisheries.noaa.gov/national/marine-mammal-protection/marine-mammal-stock-assessment-reports-region)
669 [mammal-stock-assessment-reports-region](https://www.fisheries.noaa.gov/national/marine-mammal-protection/marine-mammal-stock-assessment-reports-region).

670 National Marine Fisheries Service (NMFS). 2020. Atlantic Highly Migratory Species; Atlantic
671 Bluefin Tuna Fisheries; Pelagic Longline Fishery Management. Federal Register Document
672 No: 85 FR 18812. Available at:

673 <https://www.federalregister.gov/documents/2020/04/02/2020-06925/atlantic-highly->
674 [migratory-species-atlantic-bluefin-tuna-fisheries-pelagic-longline-fishery](https://www.federalregister.gov/documents/2020/04/02/2020-06925/atlantic-highly-migratory-species-atlantic-bluefin-tuna-fisheries-pelagic-longline-fishery).

675 Natugonza, V., C. Ainsworth, E. Sturludóttir, L. Musinguzi, R. Ogutu-Ohwayo, T. Tomasson, C.
676 Nyamweya, and G. Stefansson. 2020. Ecosystem modelling of data-limited fisheries: How
677 reliable are Ecopath with Ecosim models without historical time series fitting?. *J. Great*
678 *Lakes Res.* 46: 414–428. <https://doi.org/10.1016/j.jglr.2020.01.001>

679 Obradovich, S. G., E. H. Carruthers, and G. A. Rose. 2014. Bottom-up limits to Newfoundland
680 capelin (*Mallotus villosus*) rebuilding : the euphausiid hypothesis. *ICES J. Mar. Sci.* 71:
681 775–783.

682 Odum, W. E., and E. J. Heald. 1975. The detritus-based food web of an estuarine mangrove
683 community. *Estuar. Res. Chem. Biol. Estuar. Syst.* 1: 265–286.

684 Oksanen, J, F. G. Blanchet, M. Friendly, R. Kindt, P. Legendre, D. McGlinn, P. R. Minchin, R.
685 R. O’hara, G. L. Simpson, P. Solymos, M. H. H. Stevens, E. Szoecs, H. Wagner. 2019.
686 vegan: Community Ecology Package. R package version 2.5-6 [https://CRAN.R-](https://CRAN.R-project.org/package=vegan)
687 [project.org/package=vegan](https://CRAN.R-project.org/package=vegan)

688 Pacheco, J. C., D. W. Kerstetter, F. H. Hazin, H. Hazin, R. S. S. L. Segundo, J. E. Graves, F.
689 Carvalho, and P. E. Travassos. 2011. A comparison of circle hook and J hook performance in
690 a western equatorial Atlantic Ocean pelagic longline fishery. *Fish. Res.* 107: 39–45.
691 <https://doi.org/10.1016/j.fishres.2010.10.003>

692 Pauly, D. 1980. On the interrelationships between natural mortality, growth parameters, and
693 mean environmental temperature in 175 fish stocks. ICES J. Mar. Sci. 39: 175–192.
694 <https://doi.org/10.1093/icesjms/39.2.175>

695 Palomares, M. L., and D. Pauly. 1989. A multiple regression model for predicting the food
696 consumption of marine fish populations. Aust. J. Mar. Freshwater Res. 40: 259–273.
697 <https://doi.org/10.1071/MF9890259>

698 Perryman, H. A., J. H. Tarnecki, A. Grüss, E. A. Babcock, S. R. Sagarese, C. H. Ainsworth, and
699 A. M. Gray DiLeone. 2020. A revised diet matrix to improve the parameterization of a West
700 Florida Shelf Ecopath model for understanding harmful algal bloom impacts. Ecol. Modell.
701 416: 108890. <https://doi.org/10.1016/j.ecolmodel.2019.108890>

702 Polovina, J. J. 1984. An overview of the ECOPATH model. Fishbyte. 2: 5–7.

703 Robison, B. H. 1984. Herbivory by the myctophid fish *Ceratoscopelus warmingii*. Mar. Biol. 84:
704 119–123. <https://doi.org/10.1007/BF00392995>

705 Sagarese, S. R., M. V. Laretta, and J. F. Walter III. 2017. Progress towards a next-generation
706 fisheries ecosystem model for the northern Gulf of Mexico. Ecol. Modell. 345: 75–98.
707 <https://doi.org/10.1016/j.ecolmodel.2016.11.001>

708 Shannon, L., M. Coll, A. Bundy, D. Gascuel, J. J. Heymans, K. Kleisner, C. P. Lynam, C.
709 Piroddi, J. Tam, M. Travers-Trolet, and Y. J. Shin. 2014. Trophic level-based indicators to
710 track fishing impacts across marine ecosystems. Mar. Ecol. Prog. Ser. 512: 115–140.
711 <https://doi.org/10.3354/meps10821>

712 Shivji, M. S., J. E. Magnussen, L. R. Beerkircher, G. Hinteregger, D. W. Lee, J. E. Serafy, and E.
713 D. Prince. 2006. Validity, identification, and distribution of the Roundscale Spearfish,
714 *Tetrapturus Georgii* (Teleostei: Istiophoridae): Morphological and molecular evidence. Bull.
715 Mar. Sci. 79: 483–491.

716 Sponaugle, S., K. D. Walter, K. L. Denit, J. K. Llopiz, and R. K. Cowen. 2010. Variation in
717 pelagic larval growth of Atlantic billfishes: The role of prey composition and selective
718 mortality. Mar Biol 157: 839–849. <https://doi.org/10.1007/s00227-009-1366-z>

719 Steenbeek, J., J. Buszowski, V. Christensen, E. Akoglu, K. Aydin, N. Ellis, D. Felinto, J.
720 Guitton, S. Lucey, K. Kearney, S. Mackinson, M. Pan, M. Platts, and C. J. Walters. 2016.
721 Ecopath with Ecosim as a model-building toolbox: source code capabilities, extensions, and
722 variations. Ecol. Modell. 319: 178–189. <https://doi.org/10.1016/j.ecolmodel.2015.06.031>

723 Sutton, T. T., A. Cook, J. Moore, T. Frank, H. Judkins, M. Vecchione, M. Nizinski, and M.
724 Youngbluth. 2017. Inventory of Gulf oceanic fauna data including species, weight, and
725 measurements. *Meg Skansi* cruises from Jan. 25 - Sept. 30, 2011 in the Northern Gulf of
726 Mexico. Distributed by: Gulf of Mexico Research Initiative Information and Data
727 Cooperative (GRIIDC), Harte Research Institute, Texas A&M University-Corpus Christi.
728 <https://doi.org/10.7266/N7VX0DK2>

729 Sutton T. T., T. Frank, H. Judkins, I. C. Romero. 2020. As gulf oil extraction goes deeper, who is
730 at risk? community structure, distribution, and connectivity of the deep-pelagic fauna. In S.
731 Murawski, C. H. Ainsworth, S. Gilbert, D. J. Hollander, C. B. Paris, M. Schlüter, D. L.

732 Wetzel [eds.]. Scenarios and Responses to Future Deep Oil Spills. Springer, Cham.
733 https://doi.org/10.1007/978-3-030-12963-7_24

734 Trites, A., and D. Pauly. 1998. Estimating mean body masses of marine mammals from
735 maximum body lengths. *Can. J. Zool.* 76: 886–896. <https://doi.org/10.1139/z97-252>

736 Ulanowicz, R. 1995. Ecosystem trophic foundations: Lindeman exonerata. In: B. C. Patten, S. E.
737 Jorgensen [eds.]. *Complex Ecology: The Part–Whole Relation in Ecosystems*. 549–560.

738 Ulanowicz, R. E., and C. J. Puccia. 1990. Mixed Trophic Impacts in Ecosystems. *Coenoses*. 5:
739 7–16.

740 Walters, C., V. Christensen, and D. Pauly. 1997. Structuring dynamic models of exploited
741 ecosystems from trophic mass-balance assessments. *Rev. Fish Biol. Fish.* 7: 139–172.
742 <https://doi.org/10.1023/A:1018479526149>

743 Walters, C. J., and F. Juanes. 1993. Recruitment limitation as a consequence of natural selection
744 for use of restricted feeding habitats and predation risk taking by juvenile fishes. *Can. J. Fish.*
745 *Aquat. Sci.* 50: 2058–2070. <https://doi.org/10.1139/f93-229>

746 Watwood, S. L. P. J. O. Miller, M. Johnson, P. T. Madsen, and P. L. Tyack. 2006. Deep-diving
747 foraging behaviour of sperm whales (*Physeter macrocephalus*). *J. Anim. Ecol.* 75: 814–825.
748 <https://doi.org/10.1111/j.1365-2656.2006.01101.x>

749 Webb, T. J., B. E. Vanden, R. and O’Dor. 2010. Biodiversity’s big wet secret: the global
750 distribution of marine biological records reveals chronic under-exploration of the deep
751 pelagic ocean. *PLoS One*. 5: e10223. <https://doi.org/10.1371/journal.pone.0010223>

- 752 Wilson, S. G., and B. A. Block. 2009. Habitat use in Atlantic bluefin tuna *Thunnus thynnus*
753 inferred from diving behavior. *Endangered Species Res.* 10: 355–367.
754 <https://doi.org/10.3354/esr00240>
- 755 Worm, B., and R. A. Myers. 2003. Meta-analysis of cod-shrimp interactions reveals top-down
756 control in oceanic food webs. *Ecol.* 84: 162–173. [https://doi.org/10.1890/0012-9658\(2003\)084\[0162:MAOCSI\]2.0.CO;2](https://doi.org/10.1890/0012-9658(2003)084[0162:MAOCSI]2.0.CO;2)
- 757
- 758 Verity, P. G., and V. Smetacek. 2002. Status, trends and the future of the marine pelagic
759 ecosystem. *Environ. Conserv.* 29: 207–237. <https://doi.org/10.3354/meps130277>
- 760 Vidal, L., and D. Pauly. 2004. Integration of subsystems models as a tool toward describing
761 feeding interactions and fisheries impacts in a large marine ecosystem, the Gulf of Mexico.
762 *Ocean Coastal Manage.* 47: 709–725. <https://doi.org/10.1016/j.ocecoaman.2004.12.009>
- 763 Zeller, D., and D. Pauly. 2015. Methods-EEZ-LME-area-parameters-www.searoundus.org
764 Exclusive Economic Zones (EEZ).